

Original Research Article

Evaluation of a low-cost camera for agricultural applications

ABSTRACT

This study aimed to modify a webcam by replacing its near-infrared (NIR) blocking filter to a low-cost red, green and blue (RGB) filter for obtaining NIR images and to evaluate its performance in two agricultural applications. First, the sensitivity of the webcam to differentiate normalized difference vegetation index (NDVI) levels through five nitrogen (N) doses applied to the Batatais grass (*Paspalum notatum* Flugge) was verified. Second, images from maize crops were processed using different vegetation indices, and thresholding methods with the aim of determining the best method for segmenting crop canopy from the soil. Results showed that the webcam sensor was capable of detecting the effect of N doses through different NDVI values at 7 and 21 days after N application. In the second application, the use of thresholding methods, such as Otsu, Manual, and Bayes when previously processed by vegetation indices showed satisfactory accuracy (up to 73.3%) in separating the crop canopy from the soil.

Keywords: NDVI; Paspalum notatum fluegge; Otsu; segmentation.

1. INTRODUCTION

Recent developments in sensor technologies have made digital cameras more and more efficient and affordable. These systems have been widely used as a versatile remote sensing tool for many applications due to its advantages over film-based aerial photography and satellite imagery [1]. The main advantage of digital photography lies in simplified image processing [2]. Among the advantages of digital photography from these cameras are its relatively low cost, high spatial resolution and near-real-time availability of imagery for visual assessment and image processing.

Digital cameras are fitted with either a charge-coupled device (CCD) sensor or a complementary metal oxide semiconductor (CMOS) sensor that are photoconductive devices. These sensors are sensitive to near-infrared (NIR) wavelengths, however, most of these cameras are fitted with a blocking filter to this wavelength. Thus, typically these images present only the red, green, and blue (RGB) bands, which are sufficient to represent colors in the visible portion of the spectrum (400 – 700 nm), as recognized by the human vision [3]. In most cases, the digital photographs are recorded in joint photographic experts' group (JPEG) or tagged image file format (TIFF), and the RGB channels are obtained through image processing.

The use of images with RGB and NIR bands is very common in agricultural applications, especially for vegetation monitoring. Many vegetation indices, such as the normalized difference vegetation index (NDVI) [4] require spectral information in the NIR and red bands,

30 even though the RGB bands could be sufficient for some applications [5]. Since most
31 consumer-grade cameras only provide RGB bands, NIR filtering techniques can be used to
32 convert an RGB camera into a NIR camera. Moreover, it is possible to replace the blocking
33 filter by a long-pass infrared filter on standard CCD or CMOS sensors for obtaining NIR
34 images [6].

35 Over the years, numerous systems for collecting images based on cameras or webcams
36 have been developed and modified to obtain NIR information across multiple domains. Most
37 systems included analysis of the nutritional status of agricultural crops [7], disease detection
38 [8], yield estimation [9], and weed identification [10]. In addition, other authors highlight the
39 possibilities of using vegetation indices combined with segmentation techniques and texture
40 analysis for obtaining data of interest, such as crop canopy and soil [11, 12]. Furthermore,
41 these cameras can be mounted in a stationary installation [13] or onboard a light aircraft or
42 unmanned aerial vehicle, a deployment which was made possible due to its low weight [14,
43 15].

44 Given the many possibilities of using images from RGB or modified cameras to access the
45 NIR band, the use of artificial vision systems through image processing has enabled the
46 extraction of information of interest, which proves to be a great tool for application in the
47 agricultural environment. However, there are still factors, such as different ambient lighting
48 conditions, plant shading and complex background that are challenges to the success of
49 using low-cost images for agricultural applications as described in other studies [16, 17].
50 Therefore, in view of the challenge to obtain these images with good quality for solving
51 problems, the present study aimed to modify a webcam to obtaining data from the NIR band
52 and to evaluate its performance over different agricultural applications.

53 2. MATERIAL AND METHODS

54 The experiment was conducted at the Federal University of Viçosa, Viçosa Campus in Minas
55 Gerais, which is located among the coordinates: 20° 45' 14 "(S) and 42° 52' 54" (W), 649
56 meters above sea level. The image acquisition system comprised two C3 Tech model HB
57 2105 webcams that produced images in JPEG format (640x480 pixels).

58 In order to obtain NIR images, a modification was carried out in one of the webcams by
59 removing the NIR blocking filter, and adding an RGB blocking filter, which was made from
60 the magnetic material of a floppy disk (common diskette) as proposed by [18]. Thus, the
61 unmodified webcam, named in this study as RGB webcam and the modified NIR webcam
62 were tested on two different applications. First, the performance of the webcam's images to
63 differentiate NDVI values according to different N rates was verified. Second, these images
64 were processed for separating the crop canopy from the soil using different thresholding
65 algorithms.

66 In the first application, a field experiment was carried out using the Batatais grass (*Paspalum*
67 *notatum* Flugge), where a randomized block design with five treatments and five replications
68 was adopted. Treatments consisted of five nitrogen (N) doses in the form of ammonium
69 sulfate ((NH₄)₂SO₄), which corresponded to 0, 40, 80, 120 and 160 kg ha⁻¹. Plot dimensions
70 were 1 m × 1 m.

71 Furthermore, the digital images were captured with both webcams at a height of 3 m from
72 the ground using a ladder, with the webcam being held by one of the authors, and always
73 ensuring that the image taken cover the entire area of the experimental plot. Data acquisition
74 was performed twice with images being captured at 7 and 21 days after the N application. All
75 images were geometrically corrected through the projective transformation technique using

76 the Matlab® software, where reference points were defined at the boundaries of each plot.
77 Lastly, the NDVI [4] was calculated by Equation 1 for each experimental plot.

$$78 \quad NDVI = \frac{nir - r}{nir + r} \quad (1)$$

79 Where: nir: near-infrared band; and r: red band.

80 In addition, the portable chlorophyll meter (SPAD-502, Konica Minolta Sensing, Tokyo,
81 Japan) was used to measure the SPAD index (SI) [19]. Thus, at the 7 and 21 days after N
82 application, 30 readings per plot were taken, where the average of all readings was
83 considered as a result. In this study, the SPAD-502 readings were assumed to be the
84 reference of chlorophyll content for the purpose of validating the sensitivity of the webcams
85 in detecting the effect of N doses over the Batatais grass.

86 In order to verify the significance of the proposed treatments, the results were submitted to
87 analysis of variance (ANOVA) through the F-test. Lastly, regression models were adjusted to
88 assess treatment effects on results of the SPAD index readings and NDVI values. All
89 analyses were carried out using the ASSISTAT, version 7.7 free software [20].

90 In the second application, the RGB images were used for the ability to differentiate crop
91 canopy from soil under different growing conditions. There were 30 images captured for this
92 study and all of it belonged to maize crops at the V4 vegetative stage (four expanded
93 leaves), which were grown under different soil cover conditions, such as conventional
94 planting system, and no-tillage system with coffee husk and straw residue.

95 The digital images were captured at a height of 1.5 m from the ground and then stored as
96 24-bit colour images with resolutions of 640 × 480 pixels saved in RGB colour space in the
97 JPEG format. Then, to discriminate between the object of interest (plant) and background
98 (soil), algorithms were developed using different thresholding methods, such as Otsu [21],
99 Manual threshold selection, and Bayes [22].

100 Initially, two methods were used to accentuate the green color of plants in RGB images.
101 First, in the absolute green method, the pixel color distance (PCD) value was obtained
102 through the euclidean distance (ED) calculation using normalized values from the red and
103 green bands of each pixel, as shown in Equation 2 [23].

$$104 \quad PCD = \sqrt{pixel(r)^2 + [pixel(g) - 1]^2} \quad (2)$$

105
106 Where: r: pixel value from the red band; and g: pixel value from the green band.

107 Second, the excess green normalized index (ExG) was obtained as it is shown in Equation 3
108 [24].

$$109 \quad ExG = \frac{2 \times g - r - b}{r + g + b} \quad (3)$$

110 Where: g: pixel value from the green band; r: pixel value from the red band; and b: pixel
111 value from the blue band.

112 Subsequently, the Otsu, Manual, and Bayes methods were applied to each image. As a
113 result, all images showed some noise, which was removed by using a median filter with a

114 3 m × 3 m window size. Moreover, the ground truth segmentation model for comparison of
115 the three algorithms was developed from the K-means method.

116 Generally, this method can be employed in different areas including image processing,
117 where it can be used as a thresholding method based on data clustering. This method
118 partitions n pixels into k clusters, where k is an integer value that holds $k < n$. The k-means
119 algorithm classifies pixels in an image into k number of clusters according to some similarity
120 feature, such as the grey level intensity of pixels, and distance of pixel intensities from
121 centroid pixel intensity [25].

122 The algorithm is based on six steps:

- 123 1. Selection of k clusters (k is a user defined parameter);
- 124 2. Calculation of the number of image pixels N;
- 125 3. Selection of k initial pixel intensity centroids μ_j ;
- 126 4. Calculation of distances D_{ij} between pixel x_i and each centroid μ_j as given in Equation 4.

$$127 \quad D_{ij} = (x_i - \mu_j)^2 \quad (4)$$

129 Where: $i = 1 \div N$; and $j = 1 \div k$.

130 Particular pixel x_i is then classified to cluster c_j to which centroid it has the smallest distance.

- 132 5. Recalculation of centroid positions μ_j as a mean value of all pixel intensities, which
133 belong to cluster c_j as shown in Equation 5.

$$134 \quad \mu_j = \frac{1}{l_j} * \sum_{i=1}^{l_j} x_i \quad (5)$$

135 Where: l_j is the number of pixels that belong to cluster c_j .

- 136 6. Steps (4) and (5) are repeated until classification of the image pixels does not change.

137 In this study, the value of k (number of clusters) was defined as two, where the first
138 represented the crop canopy and second the soil. Then, in order to validate the performance
139 of each thresholding method, the accuracy index, proposed by [26] was computed using
140 Equation 6.

$$141 \quad Accuracy = 100 \times \frac{A \cap B}{A \cup B} \quad (6)$$

142 Where: A: represents the set of pixels in the ground truth image that is marked as crop
143 canopy; and; B: represents the set of pixels in the segmentation that is marked as crop
144 canopy.

145 This measure of accuracy determines how closely the segmentation matches the ground
146 truth, with 100% indicating an exact match and perfect segmentation. Thus, to verify the
147 significance of the proposed methods, the accuracy means were compared by the Students t
148 test at a 5-% significance level ($\alpha < 0.05$).

149 3. RESULTS AND DISCUSSION

150 3.1 Application 1

151 Average values of the SI and NDVI as a function of the nitrogen doses, as well as its
 152 respective coefficient of variation (CV), are shown in Table 1. It can be observed that CV
 153 values for NDVI index tended to be higher than to SI values at 7 and 21 days, which may be
 154 justified by the low uniformity of the Batatais grass on the study area. Furthermore, the fact
 155 that SPAD readings are done by direct contact with the leaf surface might have decreased
 156 its CV. In addition, its higher number of readings per plot also contributes to decrease CV
 157 values, which is not done in the NDVI calculation, since only one RGB, and NIR images are
 158 used per plot to obtain the index.

159 **Table 1. Descriptive statistics of the SI (SPAD index) and NDVI (normalized difference**
 160 **vegetation index) at 7 and 21 days after N application.**

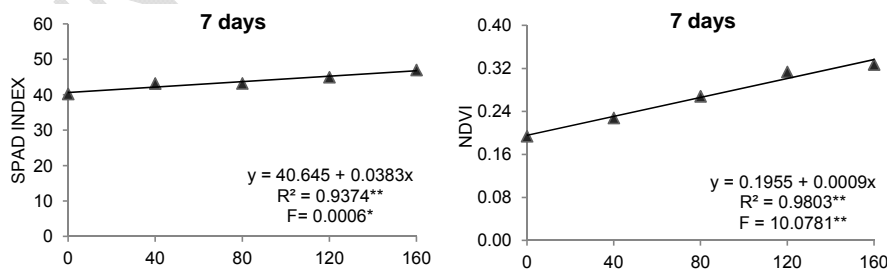
Time Days	N rates (kg ha ⁻¹)					CV (%)
	0	40	80	120	160	
SI (SPAD-502)						
7	40.22	43.17	43.20	44.95	47.00	3.67
21	37.95	44.92	48.12	45.82	46.95	6.55
NDVI (webcam)						
7	0.19	0.23	0.27	0.31	0.33	26.4
21	0.23	0.25	0.26	0.22	0.39	17.9

161 CV: Coefficient of variation

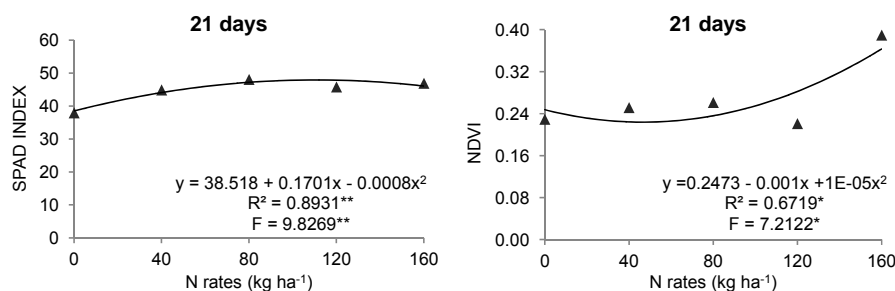
162 Even showing sensitivity to the applied N rates, NDVI results from both dates (7 and 21
 163 days) were relatively low, which might be associated with low uniformity of the vegetation,
 164 and absence of radiometric calibration. [27] highlights that using a reference panel for
 165 standardization or the inclusion of a gray Spectralon (or other diffuse reflectors) panel within
 166 the field of view of the webcam would potentially be of value for calibration under changing
 167 illumination conditions (e.g. cloudy vs. sunny days). Thus, a radiometric calibration could
 168 increase the sensitivity of the webcam, which would result in higher NDVI values and lower
 169 weather interference. However, the results obtained here suggest that even without this
 170 calibration, the webcam was still capable of detecting differences among treatments.

171 The regression analyses carried out to access the effect of nitrogen doses on SI and NDVI
 172 values at 7 and 21 day after N application showed a linear (7 days) and quadratic (21 days)
 173 response for both indices. Moreover, both indices were significant at 1% probability with a
 174 coefficient of determination (R²) of 0.93 (SI, p-value: 0.0001), and 0.98 (NDVI, p-value:
 175 0.008), respectively. In Figure 1 it is possible to observe the linear increase of the SI and
 176 NDVI values as the N doses increases at 7 days after the fertilization.

177



178



179

180 **Fig 1. SPAD Index (SI) and NDVI index as a function of topdressing nitrogen doses.**

181 When observing the SI values at 21 days (Figure 1), a linear increase in its values is also
 182 observed up to the dose of 80 kg ha⁻¹ of N. However, from the 120 kg ha⁻¹ of N, SI values
 183 showed a decrease, which demonstrates a quadratic response to different N doses with a R²
 184 of 0.8931 (p-value: 0.0068). Similarly, NDVI values showed a linear increase up to 80 kg ha⁻¹
 185 of N. Although, when looking at 120 and 160 kg. ha⁻¹ N doses, NDVI response showed a
 186 high variation for both treatments, which resulted in low correlation (R² = 0.67) (p-value:
 187 0.0169). This high variation in the NDVI response is possibly associated with the low
 188 uniformity of the grass, as well as to changes in weather and illumination conditions, which
 189 might have influenced the visual quality of the images. Even though there was a high
 190 variation in response to these treatments, SI and NDVI values at 21 days were also
 191 significant at 1%, and 5% probability, respectively.

192 In general, this quadratic response for both indices at 21 days indicates that, in this range,
 193 increasing the nutrient concentration (nitrogen) would not reflect on grass growth, and it
 194 represents the plant luxury consumption. According to [28], the luxury consumption is
 195 defined as the N storage in the vacuole instead of its participation in the chlorophyll
 196 molecule. The same authors also point out that, excessive consumption is not always
 197 undesirable since it allows plants to accumulate nutrients when its availability is high. In this
 198 case, a gradual release is performed by the plant, when the absorption is insufficient to
 199 support its growth.

200 Results obtained in this study showed that the webcam sensor evaluated was capable of
 201 detecting the effect of N doses over the Batatais grass for both dates, at 7 and 21 days after
 202 N application. The SPAD-502 used here as a reference method presented better results,
 203 which was expected due to its higher sensitivity and correlation with the leaf chlorophyll
 204 content.

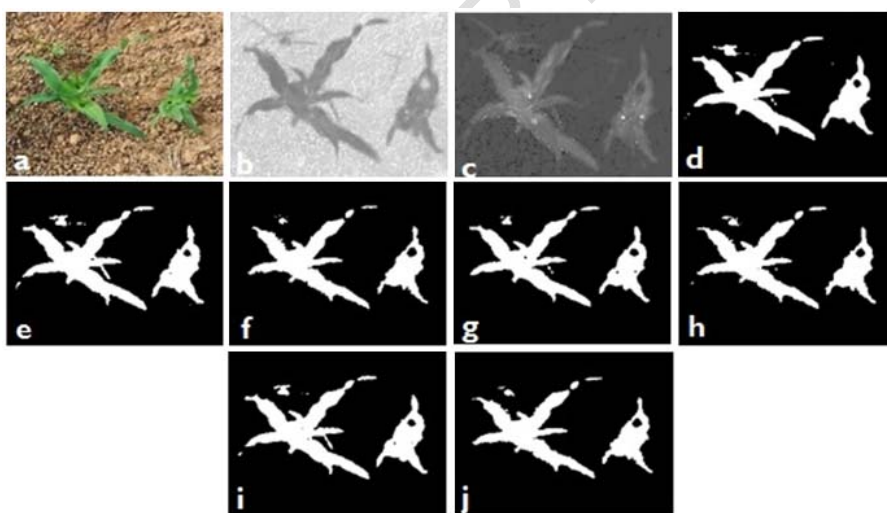
205 Compared to other low-cost, sensor-based methods for monitoring crops phenology, such as
 206 radiometric instruments based on LED sensors [29], or light emitting diodes [30], a clear
 207 advantage of using webcams is that it can yield images with good spatial resolution. This
 208 enables tracking the phenology of different crops by breaking the image into different regions
 209 of interest (e.g., crops and weeds) [27]. On the other hand, there is no doubt that higher-
 210 quality spectral imaging could, potentially, be obtained from existing, commercially available
 211 multispectral cameras. However, for budget-limited observational and experimental studies,
 212 the system proposed here may represent an acceptable compromise, given its low cost and
 213 promising performance.

214 **3.2 Application 2**

215 Initially, performance analyses of segmentation algorithms were based on visual analysis by
216 comparing the proposed methods to the reference binary image. Then, the accuracy index
217 (equation 6) was used for comparing each result with that obtained through the K-means. In
218 general, segmentation methods when combined with the ExG index showed higher accuracy
219 results than those methods preceded by the euclidean distance (ED). Moreover, the highest
220 overall mean accuracy (80.3%) was obtained using the Otsu method preceded by ExG
221 index. On the other hand, the lowest accuracy mean was observed using the Manual
222 method with the ED index (73.3%).

223 These results corroborate with [31], which observed that images segmented by the Otsu with
224 the ExG index showed 88% accuracy when compared to other indices using RGB bands. In
225 another study [32], these authors when using the Otsu method preceded by different indices,
226 such as ExG, ExR (excess of red), and another index based on the CIE l^*a^*b color space
227 obtained accuracies of 74%, 77.2%, and 62%, respectively. This demonstrates that the
228 contrast provided by vegetation indices is of great use to highlight the crop canopy from the
229 soil, and could yield in high accuracy segmentation.

230 When analyzing the accuracy of each image, the highest values were observed for the
231 Manual and Otsu method when preceded by the ED index, which resulted in 95.9% of
232 accuracy for both methods. According to [23], the ED method is based on the search for
233 homology among plants, where after obtaining the spectral energy of plant content; its
234 similarity is verified through the Euclidean distance measurement. Figure 2 shows examples
235 of resulting images from the proposed segmentation algorithms.



236 **Fig 2. Images processed by the proposed segmentation algorithms. (a) RGB image,**
237 **(b) Euclidean distance, (c) ExG index, (d) K-means, (e) Bayes with ED, (f) Bayes with**
238 **ExG, (g) Manual with ED, (h) Manual with ExG, (i) Otsu with ED, and (j) Otsu with ED.**
239

240 In order to determine the most accurate method, the data set was submitted to the Student t-
241 test at 5% significance level. Results from the ANOVA showed that statistically, there was no
242 difference in performance among the proposed methods when compared to each other.
243 Although, the highest CV values were obtained through Bayes (34.72%), and Otsu methods
244 (33.28%), when preceded by the ED index as it is shown in Table 2.

245

Table 2. Accuracy results from the proposed segmentation algorithms.

Methods	Accuracy (%)				
	Max	Min	SD	CV	Mean
Otsu + ED	95.9	32.0	25.65	33.28	77.1
Otsu + ExG	90.9	61.6	9.09	11.33	80.3
Manual + ED	95.9	32.0	23.43	31.99	73.3
Manual ExG	93.5	55.9	13.05	17.12	76.2
Bayes + ED	93.7	22.5	26.15	34.72	75.3
Bayes + ExG	90.9	61.6	16.11	21.19	76.0

246

Max: maximum; Min: minimal; SD: Standard deviation; CV: coefficient of variation. ED: Euclidean distance; ExG: Excess of green

247

248

These results can be justified by the adverse illumination conditions during the image acquisition period, which resulted in erroneous segmentation due to shaded areas in images. Thus, the Otsu, manual, and Bayes segmentation methods presented satisfactory accuracy (up to 73.3%) for separating crop canopy from the soil when preceded by the ExG and ED indices. Even though a satisfying performance has been achieved, there are still factors, such as the lighting conditions, plant shading and complex background that are challenges to the success of segmentation.

249

250

251

252

253

254

255

Thus, the application of low-cost consumer cameras for process control as an element of precision farming could save fertilizer, pesticides, machine time, and labor force. Although research activities on this topic have increased over the years, high camera prices still reflect on low adaptation to applications in all fields of agriculture. Smart cameras adapted to agricultural applications can overcome this drawback.

256

257

258

259

260

4. CONCLUSION

261

The webcam sensor was capable of detecting the effect of nitrogen doses over the Batatais grass through different NDVI values at 7 and 21 days after N application. Regarding the use of webcam images in agricultural applications through thresholding methods, it was possible to observe that the segmentation process over RGB images becomes challenging due to non-uniform illumination conditions, and complex image background. Thus, the use of thresholding methods, such as Otsu, Manual, and Bayes when previously processed by the ExG and ED indices can satisfactorily separate the crop canopy from the soil. As a recommendation for future studies, both images (NIR and RGB) can be used to calculate vegetation indexes to perform studies on phenology or plant's nutritional status. Also, the RGB images can be processed using segmentation algorithms to quantify plant diseases or leaves damaged by pests in crops.

262

263

264

265

266

267

268

269

270

271

272

COMPETING INTERESTS

273

Authors have declared that no competing interests exist.

274

AUTHORS' CONTRIBUTIONS

275

This work was carried out in collaboration between all authors. All authors read and approved the final manuscript.

276

277

REFERENCES

278

1. Yang C, Westbrook JK., Suh CPC, Martin DE, Hoffmann WC, Lan Y, & Goolsby JA. 2014. An airborne multispectral imaging system based on two consumer-grade

279

- 280 cameras for agricultural remote sensing. *Remote Sensing*, 6(6), 5257-5278. DOI:
281 <https://doi.org/10.3390/rs6065257>.
282
- 283 2. Lebourgeois V, Bégué A, Labbé S, Mallavan B, Prévot L, & Roux B. 2008. Can
284 commercial digital cameras be used as multispectral sensors? A crop monitoring
285 test. *Sensors*, 8(11), 7300-7322. DOI: <https://doi.org/10.3390/s8117300>.
286
- 287 3. Sonnentag O, Hufkens, K, Teshera-Sterne C, Young AM, Friedl M, Braswell BH,
288 Milliman T, O'keefe J, & Richardson AD. 2012. Digital repeat photography for
289 phenological research in forest ecosystems. *Agricultural and Forest Meteorology*,
290 152(1), 159–177. DOI: <https://doi.org/10.1016/j.agrformet.2011.09.009>.
291
- 292 4. Rouse JW, Haas Jr. RH, Schell JA, & Deering DW. 1974. Monitoring vegetation
293 systems in the Great Plains with ERTS, NASA SP-351. Third ERTS-1 Symposium,
294 Vol. 1, pp. 309 – 317, NASA, Washington, DC.
295
- 296 5. Nijland W, De Jong R, De Jong SM, Wulder MA, Bater CW, & Coops NC. 2014.
297 Monitoring plant condition and phenology using infrared sensitive consumer grade
298 digital cameras. *Agricultural and Forest Meteorology*, 184(1), 98-106. DOI:
299 <https://doi.org/10.1016/j.agrformet.2013.09.007>.
300
- 301 6. Rabatel G, Gorretta N, & Labbé N. 2014. Getting simultaneous red and near-
302 infrared band data from a single digital camera for plant monitoring applications:
303 Theoretical and practical study. *Biosystems Engineering*, 117(1), 2–14. DOI:
304 <https://doi.org/10.1016/j.biosystemseng.2013.06.008>.
305
- 306 7. Jia B, He H, Ma F, Diao M, Jiang G, Zheng Z, Cui J, & Fan H. 2014. Use of a digital
307 camera to monitor the growth and nitrogen status of cotton. *The Scientific World*
308 *Journal*, 2014(1), 1-12. DOI: <http://sci-hub.tw/10.1155/2014/602647>.
309
- 310 8. Castro A I, Ehsani R, Ploetz RC, Crane JH, & Buchanon S. 2015. Detection of laurel
311 wilt disease in avocado using low altitude aerial imaging. *PloS one*, 10(4), 1-13. DOI:
312 <https://doi.org/10.1371/journal.pone.0124642>.
313
- 314 9. Stroppiana D, Migliazzi M, Chiarabini V, Crema A, Musanti M, Franchino C, & Villa
315 P. 2015. Rice yield estimation using multispectral data from UAV: A preliminary
316 experiment in northern Italy. In *Geoscience and Remote Sensing Symposium*
317 *(IGARSS), IEEE International* (pp. 4664-4667). DOI:
318 <https://doi.org/10.1109/IGARSS.2015.7326869>.
319
- 320 10. Romeo J, Guerrero JM, Montalvo M, Emmi L, Guijarro M, Gonzalez-De-Santos P, &
321 Pajares G. 2013. Camera sensor arrangement for crop/weed detection accuracy in
322 agronomic images. *Sensors*, 13(4), 4348-4366. DOI: [http://sci-](http://sci-hub.tw/10.3390%2Fs130404348)
323 [hub.tw/10.3390%2Fs130404348](http://sci-hub.tw/10.3390%2Fs130404348).
324
- 325 11. Montalvo M, Guerrero JM, Romeo J, Emmi L, Guijarro M, & Pajares G. 2013.
326 Automatic expert system for weeds/crops identification in images from maize
327 fields. *Expert Systems with Applications*, 40(1), 75-82. DOI:
328 <https://doi.org/10.1016/j.eswa.2012.07.034>.
329
- 330 12. Torres-Sánchez J, López-Granados F, & Peña M. 2015. An automatic object-
331 based method for optimal thresholding in UAV images: Application for vegetation

- 332 detection in herbaceous crops. *Computers and Electronics in Agriculture*, 114(6),
333 43-52. DOI: <https://doi.org/10.1016/j.compag.2015.03.019>.
- 334
- 335 13. Sakamoto T, Shibayama M, Kimura A, & Takada E. 2011. Assessment of digital
336 camera-derived vegetation indices in quantitative monitoring of seasonal rice
337 growth. *ISPRS Journal of Photogrammetry and Remote Sensing*, 66(6), 872-882.
338 DOI: <https://doi.org/10.1016/j.isprsjrs.2011.08.005>.
- 339
- 340 14. Caturegli L, Corniglia M, Gaetani M, Grossi N, Magni S, Migliazzi M, Angelini L,
341 Mazzoncini, M, Silvestri N, Fontanelli M, Raffaelli M, Peruzzi A, & Volterrani M.
342 2016. Unmanned aerial vehicle to estimate nitrogen status of turfgrasses. *PloS one*,
343 11(6), 1-13. DOI: <https://journals.plos.org/plosone/article?id=10.1371/journal.pone.0158268>.
- 344
- 345
- 346 15. Levin N, Ben-Dor E, & Singer A. 2005. A digital camera as a tool to measure colour
347 indices and related properties of sandy soils in semiarid environments. *International*
348 *Journal of Remote Sensing*, 26(24), 5475-5492. DOI: <https://doi.org/10.1080/01431160500099444>.
- 349
- 350
- 351 16. Vesali F, Omid M, Kaleita A, & Mobli H. 2015. Development of an android app to
352 estimate chlorophyll content of corn leaves based on contact imaging. *Computers*
353 *and Electronics in Agriculture*, 116, 211-220. DOI: <https://doi.org/10.1016/j.compag.2015.06.012>.
- 354
- 355
- 356 17. Aureliano Netto AF, Martins RN, Aquino de Souza GS, Araujo GDM, Hatum de
357 Almeida SL, & Capelini VA. 2018. Segmentation of RGB images using different
358 vegetation indices and thresholding methods. *NATIVA*, 6 (4), 389-394. DOI: <http://dx.doi.org/10.31413/nativa.v6i4.5405>
- 359
- 360
- 361 18. Micha DN, Penello G, Kawabata RMS, & Camarott T. 2011. Vendo o invisível.
362 Experimentos de visualização do infravermelho feitos com materiais simples e de
363 baixo custo. *Revista Brasileira de Ensino de Física*, 33(1), 1501,2011. DOI:
364 <http://sci-hub.tw/10.1590/S1806-11172011000100015>.
- 365
- 366 19. Minolta Camera Co. Ltd. Chlorophyll meter SPAD-502 Instructional Manual. Minolta,
367 Osaka, Japan, 1989. 22p.
- 368
- 369 20. Silva FAS, & Azevedo CAV. 2016. The Assistat Software Version 7.7 and its
370 use in the analysis of experimental data. *African Journal of Agricultural*
371 *Research*, 11(39), 3733-3740. DOI:
372 <https://doi.org/10.5897/AJAR2016.11522>.
- 373
- 374 21. Otsu N. 1979. A threshold selection method from gray-level histogram. *IEEE*
375 *Transactions on System Man Cybernetics*, 9(1), 62-66. DOI:
376 <https://doi.org/10.1109/TSMC.1979.4310076>.
- 377
- 378 22. Gonzales RC, & Woods RE. 1992. Digital image processing (vol.2). Addison-
379 Wesley Publishing Company.
- 380

Field Code Changed

Formatted: Portuguese (Brazil)

Formatted: English (United States)

- 381 23. Nejati H, Azimifar Z, & Zamani M. 2008. Using fast fourier transform for
382 weed detection in corn fields. In *Systems, Man and Cybernetics. IEEE*
383 *International Conference on* (pp. 1215-1219). DOI:
384 <https://doi.org/10.1109/ICSMC.2008.4811448>.
385
- 386 24. Woebbecke DM, Meyer G.E., Von Garden K, Mortensen DA. 1995. Color
387 indices for weed identification under various soil, residue and lighting
388 conditions. *Transactions of the ASAE* 38, 259–269. DOI: [http://sci-](http://sci-hub.tw/10.13031/2013.27838)
389 [hub.tw/10.13031/2013.27838](http://sci-hub.tw/10.13031/2013.27838).
390
- 391 25. Dass R, Priyanka, Devi S. 2012. Image Segmentation Techniques.
392 *International Journal of Electronics & Communication Technology*, 3(1), 1-5.
393
- 394 26. Coy A, Rankine D, Taylor M, Nielsen DC, & Cohen J. 2016. Increasing the
395 accuracy and automation of fractional vegetation cover estimation from
396 digital photographs. *Remote Sensing*, 8(7), 474-488. DOI:
397 <https://doi.org/10.3390/rs8070474>.
398
- 399 27. Petach AR, Toomey M, Aubrecht DM, & Richardson AD. 2014. Monitoring
400 vegetation phenology using an infrared-enabled security camera. *Agricultural*
401 *and Forest Meteorology*, 195(9), 143–151. DOI:
402 <https://doi.org/10.1016/j.agrformet.2014.05.008>.
403
- 404 28. Baesso MM, de Carvalho Pinto FDA, de Queiroz D, Santos NT, & de Souza
405 Carneiro JE. 2013. Avaliação da deficiência de nitrogênio no feijoeiro
406 usando um medidor portátil de clorofila. *Engenharia na Agricultura*, 21(2),
407 122-128. DOI: <https://doi.org/10.13083/reveng.v21i2.318>.
408
- 409 29. Ryu Y, Lee G, Jeon S, Song Y, & Kimm H. 2014. Monitoring multi-layer
410 canopy spring phenology of temperate deciduous and evergreen forests
411 using low-cost spectral sensors. *Remote Sensing of Environment*, 149(6),
412 227–238. DOI: <http://sci-hub.tw/10.1016%2Fj.rse.2014.04.015>.
413
- 414 30. Ryu Y, Baldocchi DD, Verfaillie J, Ma S, Falk M, Ruiz-Mercado I, Hehn T, &
415 Sonntag O, 2010. Testing the performance of a novel spectral reflectance
416 sensor, built with light emitting diodes (LEDs), to monitor ecosystem
417 metabolism, structure and function. *Agricultural and Forest Meteorology*,
418 150(12), 1597– 1606. DOI: <https://doi.org/10.1016/j.agrformet.2010.08.009>.
419
- 420 31. Hamuda E, Glavin M, & Jones E. 2016. A survey of image processing
421 techniques for plant extraction and segmentation in the field. *Computers and*
422 *Electronics in Agriculture*, 125(7), 184-199. DOI:
423 <https://doi.org/10.1016/j.compag.2016.04.024>.
424

425 32. Bai X, Cao Z, Wang Y, Yu Z, Hu Z, Zhang X, & Li C. 2014. Vegetation
426 segmentation robust to illumination variations based on clustering and
427 morphology modelling. *Biosystems engineering*, 125(9), 80-97. DOI:
428 <https://doi.org/10.1016/j.biosystemseng.2014.06.015>.

UNDER PEER REVIEW